# Antimicrobial and antiviral activities and reaction mechanisms of an organic photocatalyst upon visible-light irradiation

Shiroma, Hayato ; Chikamoto, Atsushi ; Kameoka, Masanori ; Kumagai, Kazuo ; Matsuyama, Hideto ; Ichihashi, Yuichi

Research on Chemical Intermediates (2025) 51:2591–2604
https://doi.org/10.1007/s11164-025-05570-z

# Antimicrobial and antiviral activities and reaction mechanisms of an organic photocatalyst upon visible-light irradiation

**Hayato Shiroma[1] · Atsushi Chikamoto[1] · Masanori Kameoka[2] · Kazuo Kumagai[1,3] · Hideto Matsuyama[1,3] · Yuichi Ichihashi[1,3]**

Received: 22 January 2025 / Accepted: 19 March 2025 / Published online: 10 April 2025


## Abstract

Organic photocatalyst 9,10-dicyanoanthracene (CN-anthracene) has been demonstrated to exhibit antimicrobial activity upon visible-light irradiation. By evaluating these dependencies, this research aims to clarify the underlying mechanisms of its photocatalytic action and provide insights into its practical applications in diverse antimicrobial scenarios. This study examined the light and temperature dependence of the antimicrobial activity of CN-anthracene to further investigate its photocatalytic properties in detail. The antimicrobial activity was evaluated using the colony count method with *Escherichia coli* (*E. coli*) as the target organism. The results indicated that the antimicrobial rate increased with the light intensity and that the antimicrobial activity was above a certain level regardless of the temperature in the expected indoor temperature range. The antiviral activity of the photocatalyst was investigated using a median tissue culture infectious dose ($TCID_{50}$) assay. The results showed that the photocatalyst exhibited high viral activity against both enveloped and non-enveloped viruses. Furthermore, the presence of reactive oxygen species (·OH and $\cdot O_2^-$), which are believed to play a critical role in the observed antibacterial and antiviral activities, was confirmed. These findings demonstrate that CN-anthracene exhibits high antibacterial and antiviral activities under visible light, highlighting its potential as a novel tool for combating infectious diseases.

**Keywords** Organic photocatalysts · Visible-light irradiation · Antimicrobial activity · Antiviral activity · 9,10-Dicyanoanthracene

## Introduction

In recent years, the emergence of various viral and bacterial infectious diseases has posed significant threats to public health and resulted in substantial economic losses [1–3]. Among these, influenza virus, coxsackievirus, and *E. coli* represent critical

Extended author information available on the last page of the article

challenges due to their widespread prevalence and severe health impacts. Seasonal influenza affects an estimated 1 billion people annually, with 290,000–650,000 respiratory deaths worldwide [4]. Coxsackieviruses, which are associated with myocarditis, meningitis, and hand-foot-and-mouth disease (HFMD), account for over 2 million cases annually in the Asia–Pacific region [5]. Additionally, *E. coli*, a common bacterial pathogen, is a major cause of foodborne illnesses and healthcare-associated infections, leading to significant morbidity and mortality globally [6]. To address these challenges, the development of innovative and efficient disinfection technologies has become an urgent necessity. Among such technologies, photocatalysis has garnered significant attention due to its ability to utilize light energy for antimicrobial and antiviral applications. Titanium dioxide, a widely studied oxide semiconductor, undergoes electronic excitation when exposed to light energy surpassing its band gap. This process promotes electrons from the valence band to the conduction band, resulting in the generation of electron–hole pairs [7–14]. These electrons and holes diffuse to the surface, where they undergo oxidation and reduction reactions with adsorbed substances. Reports indicate that this redox process produces reactive oxygen species (ROS) with extremely high oxidizing power, such as hydroxyl radicals (·OH), superoxide anion radicals ($\cdot O_2^-$), and hydrogen peroxide [15, 16]. Because these bacteria and viruses are sterilized through oxidation and structural destruction, semiconductor photocatalysts are expected to play a significant role in antibacterial and hygienic applications. However, conventional antibacterial and antiviral photocatalysts, such as titanium dioxide, rely on ultraviolet light as an energy source for sterilization [15, 17]. While ecological considerations favor using sunlight as an energy source for photocatalysts, ultraviolet light constitutes only a small fraction of sunlight, with visible light comprising the majority. Consequently, there is an urgent need to develop photocatalysts capable of absorbing visible light, which dominates sunlight, as an alternative to titanium dioxide, which primarily absorbs ultraviolet light [18].

Organic semiconductors, particularly in electronics, are being actively researched and developed for advanced electronic devices such as solar cells, light-emitting diodes, and transistors [19–21]. These materials are also gaining attention as potential photocatalysts [8, 22–25].

The highest occupied molecular orbital (HOMO) and lowest unoccupied molecular orbital (LUMO) of organic photocatalysts correspond to the valence and conduction bands of inorganic semiconductors, respectively [26]. The HOMO and LUMO levels play a crucial role in photocatalytic reactions. The wavelength of light necessary to drive the reaction is determined by the HOMO–LUMO energy gap, which must be minimized to achieve visible-light responsiveness in photocatalytic processes. The HOMO and LUMO levels of organic semiconductors can be tuned by introducing substituents. Quantum chemical simulations using Density Functional Theory (DFT) calculations were employed to predict these energy levels. Consequently, the HOMO and LUMO energy levels can be precisely adjusted, facilitating the development of new photocatalysts with visible-light responsivity [27].

Leveraging this tunability, CN-anthracene, a polycyclic aromatic compound, has been reported to function as a photocatalyst under visible light and exhibit high antibacterial activity against *E. coli* [28]. However, while certain findings have been

obtained regarding antimicrobial activity and photocatalytic properties, the effects of environmental factors such as light intensity and temperature on the antimicrobial effect have not been fully investigated. Clarification of these dependencies will enable identification of optimal reaction conditions and a better understanding of the functional mechanism as a photocatalyst, as well as the setting of specific conditions for practical use.

In this study, we evaluated the antimicrobial activity of CN-anthracene by examining its dependence on light intensity and temperature to further explore its photocatalytic properties. The antiviral activity of CN-anthracene was investigated using the $TCID_{50}$ method, targeting Influenza A virus (an enveloped virus) and Coxsackievirus B3 (a non-enveloped virus). Additionally, the presence of ROS, such as ·OH and $\cdot O_2^-$, which are believed to contribute to antimicrobial and antiviral effects [29, 30], was confirmed.

## Materials and methods

### Materials

CN-anthracene (> 98.0%) and 5,5-dimethyl-1-pyrroline N-oxide (DMPO) were purchased from Tokyo Chemical Industry (Tokyo, Japan). Methanol (> 99.8%), isopropyl alcohol (IPA) (> 99.7%), and superoxide dismutase (SOD) were purchased from Nacalai Tesque (Kyoto, Japan). All reagents utilized in this study were of analytical grade and used directly without any additional purification. Deionized water and acetone were employed as the solvents for all experimental procedures. The crystallinity of commercially available CN-anthracene was confirmed by X-ray diffraction (XRD), as shown in Fig. S1. Several sharp diffraction peaks were observed, with calculated interplanar spacings of 8.5 Å, 8.1 Å, 7.1 Å, 4.3 Å, 4.0 Å, 3.5 Å, and 3.3 Å. These values correspond to different crystal planes, consistent with the characteristics of molecular crystals. Additionally, FT-IR measurements (Fig. S2) revealed a sharp peak around 2220 $cm^{-1}$, confirming the presence of the cyano group.

### Light intensity dependence of antimicrobial activity

The antibacterial activity experiments were conducted using *E. coli* (NBRC3301). The preparation and evaluation processes were as follows:

Ion-exchanged water (300 mL), agar powder (4.5 g), and LB medium powder (6 g) were combined in triangular flasks and sterilized by autoclaving at 121 °C for 20 min. After cooling at room temperature for 2 h, the sterilized mixture was dispensed into plastic Petri dishes under a clean bench environment and allowed to solidify, forming LB agar medium.

A platinum loop was employed to collect *E. coli*, which was inoculated onto the solidified LB agar medium using the preparative culture method. The plates were incubated overnight at 37 °C. A single colony from the resulting culture was

subsequently transferred with a platinum loop into LB liquid medium and incubated at 37 °C overnight under shaking conditions. The overnight *E. coli* culture was diluted 1000-fold in sterilized saline within an autoclaved container to produce a stock solution, referred to as Sample A.

For the photocatalytic experiments, a quartz tube reactor with a total volume of 5.9 mL was prepared. The reactor was filled with 4 mL of Sample A, containing *E. coli* at a concentration of $10^5$–$10^6$ CFU/mL, and either CN-anthracene ($3 \times 10^{-5}$ mol) or a mock treatment (without photocatalyst). The samples were irradiated with 340 nm light at intensities of 0.05, 0.20, 0.40, and 0.80 W/m$^2$, and with 560 nm light at intensities of 0.16, 0.63, 1.3, and 2.5 W/m$^2$. Following light exposure, the samples were diluted 100-fold with saline, and 20 µL of the diluted solution was plated onto LB agar medium. The plates were incubated overnight at 37 °C, and the number of bacterial colonies was subsequently counted.

The number of viable bacteria before and after the photocatalytic treatment was recorded as $N_0$ and N, respectively. The antimicrobial activity was quantified using the following formula:

$$\text{Antimicrobial activity} = \left(1 - \frac{N}{N_0}\right) \times 100\%$$

### Temperature dependence of antimicrobial activity

A 4 mL suspension ($10^5$–$10^6$ CFU/mL) of previously described *E. coli* A and CN-anthracene ($3 \times 10^{-5}$ mol) was transferred into a 5.9 mL quartz tube reactor. The reactor was secured in a cooling water circulation system and irradiated for 2 h using a fluorescent lamp. The temperatures were set to 5 °C, 15 °C, 25 °C, and 40 °C at a measured light intensity of 0.6 W/m$^2$ using a 340 nm light meter, while the corresponding intensity at 560 nm was 1.90 W/m$^2$. After irradiation, the solution was applied to the LB agar medium under the same conditions as those mentioned above, and the antibacterial rate was determined.

### Cells and virus

MDCK cells were cultured in Eagle's minimal essential medium (MEM1, Nissui Pharmaceutical Co., Ltd., Tokyo, Japan) supplemented with 10% FBS, while HeLa cells were maintained in Dulbecco's modified Eagle's medium (DMEM) (Nacalai Tesque) supplemented with 10% FBS in a $CO_2$ incubator. The Influenza A H1N1 strain, A/Puerto Rico/8/1934, was propagated in MDCK cells cultured in FBS-free MEM supplemented with 2 µg/mL acetylated trypsin (Sigma-Aldrich, Merck, Kenilworth, New Jersey, USA) for three days. Coxsackievirus B3 strain Nancy was propagated in HeLa cells cultured in DMEM supplemented with 10%

FBS for three days. Viral supernatants were clarified by centrifugation, aliquoted, and stored at − 85 °C.

### Antiviral experiments with CN-anthracene

Viral supernatants were adjusted to the appropriate tissue culture infection dose ($TCID_{50}$), mixed with CN-anthracene, and irradiated with visible light for a fixed duration. The reaction conditions are detailed in Table 1. Coxsackievirus, a non-enveloped virus, exhibits greater resistance to alcohol and is also suggested to have relatively higher tolerance to reactive oxygen species compared to the enveloped influenza virus. To observe a more distinct inactivation effect, a higher photocatalyst concentration was used for coxsackievirus. Additionally, while coxsackievirus remains stable at room temperature for several hours, influenza virus undergoes natural inactivation under the same conditions. Therefore, the influenza virus experiments were conducted at 0 °C to eliminate temperature-induced inactivation effects. A 500 W xenon lamp served as the light source, with the light controlled using a color glass filter (HOYA UV-42). The light intensity was measured at 40 $W/m^2$ using a photometer at 340 nm. Experiments conducted in ambient light were performed using fluorescent room light on the virus solution in a glass reactor without a specialized light source. A 340 nm photometer was used to measure the light intensity, which was determined to be 0.80 $W/m^2$, while the corresponding intensity at 560 nm was 2.5 $W/m^2$. After light irradiation, the virus solution was serially diluted in tenfold increments and incubated with MDCK or HeLa cells for three days for virus titration. The cells were then fixed with 5% formaldehyde in phosphate-buffered saline (PBS) and stained with 0.5% crystal violet in 20% EtOH. After staining with 0.5% crystal violet in 20% EtOH, $TCID_{50}$ was calculated using the Spearman-Kärber method.

### DMPO spin-trapping experiment

Electron spin resonance spectroscopy (ESR, BRUKER-EMX-plus, Japan) was employed to investigate the formation mechanisms of hydroxyl radicals (·OH) and superoxide radicals ($\cdot O_2^-$). An aqueous methanol solution (80 vol%) was used owing to the high dielectric constant of water. CN-anthracene was added to the methanol solution and adjusted to 7.5 mM. To this solution, 0.01 g of DMPO was added as a spin-trapping agent. The aqueous solution was irradiated with light for a fixed period of 20 min with continuous stirring. A 500 W xenon lamp served

**Table 1** Reaction conditions

| Target virus | Catalyst concentration (mM) | Temperature (℃) |
|---|---|---|
| Influenza virus | 15 | 0 |
| Coxsackievirus | 30 | 25 |

as the light source, with the light wavelength controlled using a HOYA UV-42 colored glass filter to remove light below 420 nm.

## Results and discussion

### Light and temperature dependence of the antibacterial activity of CN-anthracene

The predicted mechanism of this reaction is as follows: electrons ($e^-$) excited upon light irradiation reduce oxygen to produce hydrogen peroxide, while holes ($h^+$) generated by excitation oxidize water to produce oxygen. Titanium dioxide photocatalysts are known to generate and disinfect hydrogen peroxide and ROS, including superoxide anion radicals ($\cdot O_2^-$) and hydroxyl radicals ($\cdot OH$), are generated during this process. Additionally, hydrogen peroxide is known to play a significant role in microbial disinfection.

Reduction of oxygen by excited electrons

$$O_2 + e^- \rightarrow \cdot O_2^-$$

$$\cdot O_2^- + H^+ \rightarrow HO_2\cdot$$

$$HO_2 \cdot + H^+ + e^- \rightarrow H_2O_2$$

Oxidation of water by pores

$$2H_2O + 2h^+ \rightarrow 2 \cdot OH + 2H^+$$

$$2 \cdot OH + 2h^+ \rightarrow O_2 + 2H^+$$

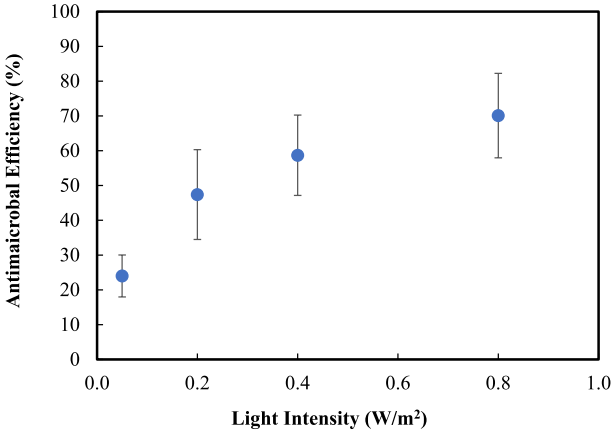


**Fig. 1** Antimicrobial efficiency of CN-anthracene against *E. coli* upon room light irradiation for 2 h

**Table 2** Temperature dependence of the antimicrobial activity of CN-anthracene upon room light irradiation

| Temperature (°C) | Antibacterial efficiency (%) |
|---|---|
| 5 | 44 |
| 15 | 54 |
| 25 | 53 |
| 40 | 47 |

**Table 3** Antiviral activity of CN-anthracene upon visible-light irradiation

| Irradiation time (h) | $TCID_{50}$ ($TCID_{50}$/mL) | |
|---|---|---|
| | Photocatalyst/light | Photocatalyst/dark |
| 0 | $2.0\times10^{7}$ | $2.0\times10^{7}$ |
| 3 | N.D.[a] | $1.3\times10^{5}$ |

[a]N.D. refers to "Not Detected"

Figure 1 shows the light intensity dependence of the antibacterial activity of CN-anthracene, indicating a positive correlation between light intensity and antibacterial activity. This result suggests that CN-anthracene exhibits photocatalytic antibacterial activity via a mechanism similar to that of titanium dioxide photocatalysts. The initial rapid decrease in bacterial population could be attributed to a sufficient supply of ROS, which efficiently inactivates bacteria at the early stage. However, as bacterial numbers decrease over time, the interaction between ROS and bacterial surfaces diminishes, leading to a reduction in overall antibacterial efficiency. Table 2 shows the results of the temperature dependence of the antimicrobial activity of CN-anthracene; it was found that in the expected indoor temperature range of 5–40 °C, the antimicrobial activity remained above a certain threshold, regardless of the temperature. Although an increase in the reaction rate would typically lead to higher antimicrobial activity with increasing temperature, the activity decreased by 6% at 40 °C. This decline may be attributed to the high reactivity of ROS. At elevated temperatures, ROS likely become less stable, resulting in a shorter lifetime. Additionally, the solubility of oxygen, the precursor of ROS, may have decreased at higher temperatures. The inactivation mechanism of *E. coli* by photocatalysts has been reported by Carré et al. [31], and a similar mechanism is considered to be involved in this study.

## Evaluation of antiviral activity of CN-anthracene against influenza virus

Table 3 shows the results of the evaluation of the antiviral performance of CN-anthracene against the influenza virus. In the absence of light, the $TCID_{50}$ value of the virus decreased to $1.3\times10^{5}$ ($TCID_{50}$/mL) within 3 h after the introduction of the photocatalyst, indicating that the virus was inactivated by factors such as adsorption onto the photocatalyst surface. When the photocatalyst was introduced and irradiated with visible light, the $TCID_{50}$ value dropped below the detection limit of

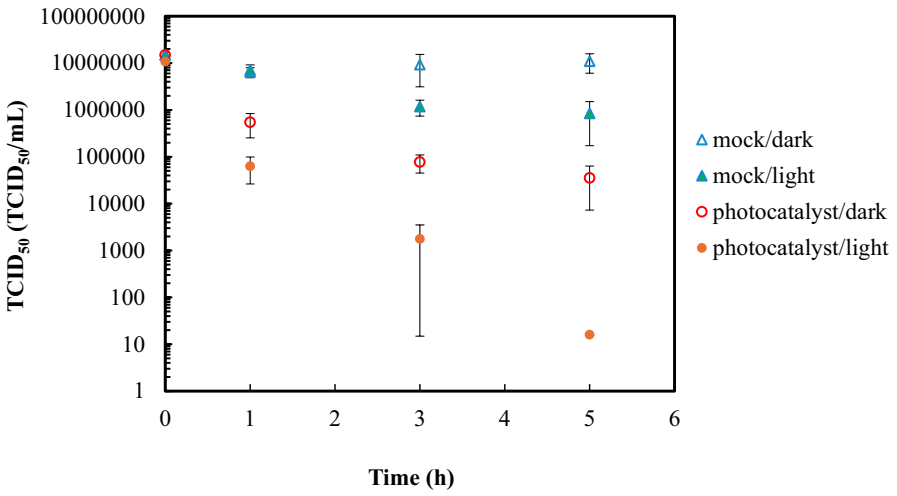


**Fig. 2** Antiviral activity against the influenza virus with or without the catalyst upon room light irradiation

$1.3 \times 10^2$ $TCID_{50}$/mL within the same period. This suggests that CN-anthracene is minimally toxic and exhibits high photocatalytic antiviral activity upon visible-light irradiation. Figure 2 illustrates the inactivation experiments conducted under practical conditions using fluorescent room light. The $TCID_{50}$ values of the influenza viruses remained relatively unchanged in the photocatalyst/dark, mock/light, and mock/dark groups, but decreased significantly in the photocatalyst/light group as the irradiation time increased. These findings demonstrate that CN-anthracene efficiently inactivates viruses not only upon visible-light irradiation but also under mild indoor lighting conditions.

### Evaluation of antiviral activity of CN-anthracene against coxsackievirus

The results of the evaluation of the antiviral performance of CN-anthracene against coxsackieviruses upon visible-light irradiation are shown in Fig. 3. Similar to the influenza virus inactivation experiment, the viral infectivity titer remained unchanged in the photocatalyst/dark, mock/light, and mock/dark groups, but decreased with increasing irradiation time in the photocatalyst/light group.

As shown in Table 4, the virus was inactivated upon ambient light irradiation. These results demonstrate that CN-anthracene photocatalytically inactivates a range of pathogens. These pathogens exhibit differences in genomic characteristics, such as genome type (DNA or RNA), genome length, and segmentation (single or multiple segments), as well as in virion structure, including the presence or absence of an envelope. The results demonstrated that ROS generated by photocatalysis exhibited antiviral activity regardless of the structural differences among pathogens. However, there was a significant variation in the time required for inactivation, with

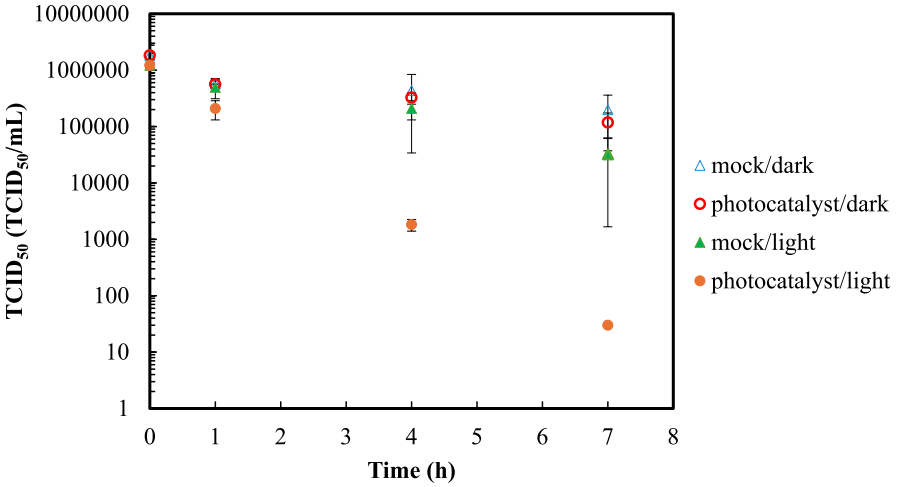


**Fig. 3** Antiviral activity against the coxsackievirus with or without visible-light irradiation (λ > 420 nm)

**Table 4** Antiviral activity of CN-anthracene upon room light irradiation

| Irradiation Time (h) | $TCID_{50}$ ($TCID_{50}$/mL) | | | |
|---|---|---|---|---|
| | Photocatalyst/light | Photocatalyst/dark | Mock/light | Mock/dark |
| 0 | $4.2 \times 10^5$ | $4.2 \times 10^5$ | $4.2 \times 10^5$ | $4.2 \times 10^5$ |
| 24 | N.D.[a] | $9.2 \times 10^4$ | $4.8 \times 10^3$ | $8.3 \times 10^4$ |

[a]N.D. refers to "Not Detected"

coxsackievirus showing greater resistance to ROS compared to influenza virus. Two primary factors may account for this difference.

First, differences in viral outer structures influence resistance. The basic structure of a virus consists of a capsid (a protein shell enclosing the genetic material) and, in some cases, an envelope (a lipid bilayer). The envelope, derived from the host cell membrane, facilitates viral entry into host cells but is chemically unstable and highly susceptible to oxidative damage. As an enveloped virus, influenza virus loses its infectivity when its membrane is damaged, making it more vulnerable to ROS-induced inactivation [32]. In contrast, coxsackievirus, a non-enveloped virus, lacks this fragile membrane, and its capsid is directly exposed to the environment. The capsid is composed of relatively stable proteins, which are less susceptible to ROS-induced damage.

Second, genome length may influence viral resistance. ROS can also damage viral genomes, and the probability of oxidative damage generally increases with genome length. Influenza virus possesses a relatively long RNA genome (~13,500 nucleotides), making it more susceptible to oxidative stress, whereas

coxsackievirus has a shorter RNA genome (~7400 nucleotides), potentially reducing its risk of oxidative damage [33].

These findings suggest that coxsackievirus exhibits higher ROS resistance than influenza virus due to its stable capsid structure and shorter genome length, which together contribute to its greater resilience against oxidative stress.

## Characterization of ROS

During photocatalysis, ROS containing ·OH and $\cdot O_2^-$, which are harmful to pathogens [34], are generated. ROS formation was quantified through DMPO spin-trap ESR spectroscopy. A characteristic peak of the ROS was observed after 20 min of visible-light irradiation (40 W/m$^2$, 340 nm). Next, 10 mM isopropyl alcohol (IPA) and 1 mg/mL superoxide dismutase (SOD) were added to the solutions

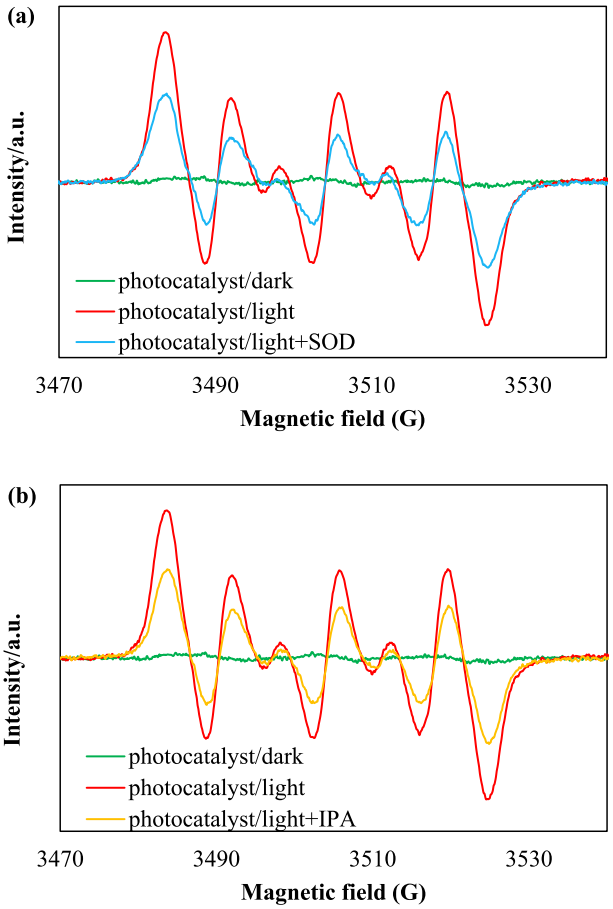


**Fig. 4** ESR spectra of ROS detected by DMPO spin-trapping of CN-anthracene irradiated for 20 min, with or without SOD (**a**) and IPA (**b**) as the quenching agent

**Table 5** Antiviral activity of CN-anthracene in the presence or absence of the quenching agents against influenza virus upon visible-light irradiation for 1 h

| | $TCID_{50}$ ($TCID_{50}$/mL) |
|---|---|
| Photocatalyst/light | $1.3 \times 10^3$ |
| Photocatalyst/light + IPA | $7.5 \times 10^4$ |
| Photocatalyst/light + SOD | $4.2 \times 10^3$ |

containing ·OH and $\cdot O_2^-$. The intensity of the ROS-derived peaks was reduced in both cases (Fig. 4a, b).

The results suggest that the CN-anthracene photocatalyst can generate ROS, such as ·OH and $\cdot O_2^-$, upon visible-light irradiation. Photocatalytic inactivation experiments were then performed in the presence of 10 mM IPA or 1 mg/ml SOD.

The results showed that the anti-influenza virus effect of light-irradiated CN-anthracene was more markedly inhibited by the ·OH quencher IPA than by the $\cdot O_2^-$ quencher SOD (Table 5). This suggests that ·OH radicals play a more dominant role in the anti-influenza virus activity.

This phenomenon can be attributed to the fact that compared to $\cdot O_2^-$, ·OH are short-lived (with a lifetime of approximately $10^{-9}$ seconds in biological systems) and highly reactive, immediately reacting with surrounding molecules and exerting strong oxidative effects on cellular components such as lipids, proteins, and nucleic acids [35]. Furthermore, ·OH is a neutral radical, unlike $\cdot O_2^-$, which carries a negative charge. Radicals with a negative charge, such as $\cdot O_2^-$, have limited mobility in aqueous environments and within hydrophobic structures such as viral envelopes. In contrast, ·OH, being neutral, can readily diffuse through both the envelope and the capsid [36, 37]. This property allows ·OH to attack various viral structures more efficiently, thereby significantly contributing to viral inactivation.

## Conclusion

We demonstrated that CN-anthracene organic photocatalysts exhibit photocatalytic inactivation of both bacteria and viruses, with ROS likely contributing to this inactivation. Most notably, these photocatalysts can induce reactions under visible light alone or even under low-intensity illumination, such as indoor lighting. Furthermore, as organic compounds, these photocatalysts exhibit high affinity for organic materials, including plastics and textiles, making them particularly suitable for applications in medical devices. This characteristic, combined with their ability to function under mild conditions, provides significant advantages over conventional sterilization methods such as heat, ultraviolet radiation, detergents, and ethanol [38, 39]. However, further research is required to assess the long-term stability of photocatalysts and their effectiveness over repeated use, which are critical for practical applications. Additionally, a comprehensive evaluation of performance and safety under real-world conditions remains an important subject for future studies.

Through further optimization and validation, these materials may contribute to the development of more effective and versatile disinfection strategies.

**Supplementary Information** The online version contains supplementary material available at https://doi.org/10.1007/s11164-025-05570-z.

**Acknowledgements** The authors would like to thank Editage (www.editage.com) for English language editing.

**Author contribution** Hayato Shiroma: Methodology, Investigation, Writing—Original Draft Atsushi Chikamoto: Investigation, Writing—Original Draft Masanori Kameoka: Methodology, Investigation, Writing—Original Draft Kazuo Kumagai: Investigation, Resources Hideto Matsuyama: Investigation, Resources Yuichi Ichihashi: Supervision, Conceptualization, Project administration, Funding acquisition, Methodology, Writing—Original Draft.

**Funding** Open Access funding provided by Kobe University. This work was supported by JSPS KAKENHI (grant number22K04827).

**Data availability** No datasets were generated or analysed during the current study.

## Declarations

**Competing interests** The authors declare that they have no known competing financial interests or personal relationships that could have appeared to influence the work reported in this paper.

**Ethics approval** Not applicable.



## References

1. M.M. Al-Abdallat, D.C. Payne, S. Alqasrawi, B. Rha, R.A. Tohme, G.R. Abedi, M. AlNsour, I. Iblan, N. Jarour, N.H. Farag, A. Haddadin, T. Al-Sanouri, A. Tamin, J.L. Harcourt, D.T. Kuhar, D.L. Swerdlow, D.D. Erdman, M.A. Pallansch, L.M. Haynes, S.I. Gerber, N. Sabri, M. AlAzhari, H. Khazali, M. AlMaayah, A. Bilbeisi, N. Dawood, B. AlZubi, J. Meflih, T. Mounds, J. Fitzner, A. Eltom, A. Mafi, C. Miao, H. Caidi, S. Trivedi, S. Kamili, A.J. Hall, A. Curns, J. Moore, H. Pham, C. Zimmerman, E. Farnon, G. Giorgi, R. Gerber, ftJM-CI Team, Clin. Infect. Dis. **59**, 1225 (2014)
2. A. Choi, A. García-Sastre, in *Microbial Forensics*, 3rd edn., Academic Press, pp. 89–104 (2014).
3. A. Du Toit, Nat. Rev. Microbiol. **18**, 123 (2020)
4. A.D. Iuliano, K.M. Roguski, H.H. Chang, D.J. Muscatello, R. Palekar, S. Tempia, C. Cohen, J.M. Gran, D. Schanzer, B.J. Cowling, P. Wu, J. Kyncl, L.W. Ang, M. Park, M. Redlberger-Fritz, H. Yu, L. Espenhain, A. Krishnan, G. Emukule, L. van Asten, S.P. da Silva, S. Aungkulanon, U. Buchholz, M.-A. Widdowson, J.S. Bresee, Lancet **391**, 1285 (2018)
5. T. Solomon, P. Lewthwaite, D. Perera, M.J. Cardosa, P. McMinn, M.H. Ooi, Lancet Infect. Dis. **10**, 778 (2010)

6. E. Scallan, R.M. Hoekstra, F.J. Angulo, T.F. Jones, M.A. Widdowson, S.L. Roy, J.L. Jones, P.M. Griffin, Emerg. Infect. Dis. **17**, 7 (2011)
7. M.D. D'Arienzo, J. Carbajo, A. Bahamonde, M. Crippa, S. Polizzi, R. Scotti, L. Wahba, F. Morazzoni, J. Am. Chem. Soc. **133**, 17652 (2011)
8. A. Okemoto, K. Tanaka, Y. Kudo, S. Gohda, Y. Koshiba, K. Ishida, T. Horie, K. Taniya, Y. Ichihashi, S. Nishiyama, Catal. Today **307**, 231 (2018)
9. U.I. Gaya, A.H. Abdullah, J. Photochem. Photobiol. C **9**, 1 (2008)
10. K. Obata, K. Kishishita, A. Okemoto, K. Taniya, Y. Ichihashi, S. Nishiyama, Appl. Catal. B **160–161**, 200 (2014)
11. U. Baig, M.A. Ansari, M.A. Gondal, S. Akhtar, F.A. Khan, W.S. Falath, Mater. Sci. Eng. C **113**, 110992 (2020)
12. B. Kim, D. Kim, D. Cho, S. Cho, Chemosphere **52**, 277 (2003)
13. D.H. Song, S.H. Uhm, S.E. Kim, J.S. Kwon, J.G. Han, K.N. Kim, Mater. Res. Bull. **47**, 2994 (2012)
14. M.N. Chong, B. Jin, C.W.K. Chow, C. Saint, Water Res. **44**, 2997 (2010)
15. Z. Xiangkang, L. Yue, Y. Xia, U. Hamayet, X. Dehua, M. David, D. Ana, Y. Jiaguo, Z. Xiwang, Appl. Catal. B **5**, 119095 (2020)
16. H. Pant, B. Pant, R.K. Sharma, A. Amarjargal, H.J. Kim, C.H. Park, L. Tijing, C.S. Kim, Ceram. Int. **2**, 1503 (2013)
17. H. Sun, T. Peng, B. Liu, H. Xian, Appl. Clay Sci. **114**, 440 (2015)
18. S. Dong, L. Cui, W. Zhang, L. Xia, S. Zhou, C.K. Russell, M. Fan, J. Feng, J. Sun, Chem. Eng. J. **384**, 123279 (2020)
19. S. Naserian, M. Izadyar, E. Ranjbakhsh, J. Photochem. Photobiol. A **435**, 114283 (2023)
20. G. Gelinck, P. Heremans, K. Nomoto, T.D. Anthopoulos, Adv. Mater. **22**, 3778 (2010)
21. A.F. Paterson, S. Singh, K.J. Fallon, T. Hodsden, Y. Han, B.C. Schroeder, H. Bronstein, M. Heeney, I. McCulloch, T.D. Anthopoulos, Adv. Mater. **30**, e1801079 (2018)
22. J.T. Kintigh, J.L. Hodgson, A. Singh, C. Pramanik, A.M. Larson, L. Zhou, J.B. Briggs, B.C. Noll, E. Kheirkhahi, K. Pohl, N.E. McGruer, G.P. Miller, A. Robust, J. Phys. Chem. **118**, 26955 (2014)
23. H. Sun, A. Putta, M. Billion, J. Phys. Chem. A **116**, 8015 (2012)
24. A. Okemoto, K. Kishishita, S. Maeda, S. Gohda, M. Misaki, Y. Koshiba, K. Ishida, T. Horie, K. Taniya, Y. Ichihashi, S. Nishiyama, Appl. Catal. B **192**, 88 (2016)
25. Y. Ichihashi, T. Sekiguchi, Y. Tokui, R. Hori, S. Naito, Y. Koshiba, Y. Sutani, K. Ishida, K. Taniya, S. Nishiyama, Catal. Today **410**, 317 (2023)
26. A. Ibhadon, P. Fitzpatrick, Catalysts **3**, 189 (2013)
27. T. Oya, E. Kusano, Vacuum **83**, 564 (2008)
28. Y. Ichihashi, T. Sekiguchi, K. Hiramatsu, Y. Tokui, K. Kumagai, H. Matsuyama, K. Taniya, S. Nishiyama, Appl. Cat. B. **325**, 122326 (2023)
29. H.N. Pham, T. McDowell, E. Wilkins, J. Environ. Sci. Health Part A-Environ. Sci. Eng. Toxic Hazard. Subt. Control **30**, 627 (1995)
30. M. Wainwright, Int. J. Antimicrob. Agents **21**, 510 (2003)
31. G. Carré, E. Hamon, S. Ennahar, M. Estner, M.-C. Lett, P. Horvatovich, J.-P. Gies, V. Keller, N. Keller, P. Andre, Appl. Environ. Microbiol. **80**, 2573 (2014)
32. R. Yokohata, Y. Ishida, M. Nishio, T. Yamamoto, T. Mori, F. Suzuki, M. Hasumi, T. Okano, T. Morimoto, K. Fuji, Jpn. J. Risk Anal. **30**, 5 (2020)
33. Y. Tonga, G. Shi, G. Hu, X. Hu, L. Han, X. Xie, Y. Xu, R. Zhangc, J. Sun, J. Zhonga, Chem. Eng. J. **414**, 128788 (2021)
34. X. Yu, S. Wang, X. Zhang, A. Qi, X. Qiao, Z. Liu, M. Wu, L. Li, Z. Wang, Nano Energy **46**, 29 (2018)
35. M. Alanazi, M.A. Alamry, F. Alharthi, H.U. Rehman, Chem. Asian J. **19**, e202400105 (2024)
36. B. Halliwell, J.M.C. Gutteridge, *Free Radical Biology and Medicine*, 4th edn. (Oxford University Press, Oxford, 2007)
37. T. Na, Y. Wang, H. Wang, J. Zhang, L. Li, Chem. Commun. **47**, 12318 (2011)
38. S. Pfaender, J. Brinkmann, D. Todt, N. Riebesehl, J. Steinmann, J. Steinmann, T. Pietschmann, E. Steinmann, Appl. Environ. Microbiol. **81**, 1616 (2015)
39. M. Galasso, J.J. Feld, Y. Watanabe, M. Pipkin, C. Summers, A. Ali, R. Qaqish, M. Chen, R.V.P. Ribeiro, K. Ramadan, L. Pires, V.S. Bagnato, C. Kurachi, V. Cherepanov, G. Moonen, A. Gazzalle, T.K. Waddell, M. Liu, S. Keshavjee, B.C. Wilson, A. Humar, M. Cypel, Nat. Commun. **10**, 481 (2019)

## Authors and Affiliations

**Hayato Shiroma[1] · Atsushi Chikamoto[1] · Masanori Kameoka[2] · Kazuo Kumagai[1,3] · Hideto Matsuyama[1,3] · Yuichi Ichihashi[1,3]**

✉ Yuichi Ichihashi
ichiy@kobe-u.ac.jp

Hayato Shiroma
maroshi0402@icloud.com

Atsushi Chikamoto
2164738t@stu.kobe-u.ac.jp

Masanori Kameoka
mkameoka@port.kobe-u.ac.jp

Kazuo Kumagai
k.kumagai@port.kobe-u.ac.jp

Hideto Matsuyama
matuyama@kobe-u.ac.jp

[1] Department of Chemical Science and Engineering, Graduate School of Engineering, Kobe University, Rokkodai, Nada, Kobe 657-8501, Japan

[2] Department of Public Health, Kobe University Graduate School of Health Sciences, Tomogaoka, Suma, Kobe 654-0142, Japan

[3] Research Center for Membrane and Film Technology, Graduate School of Engineering, Kobe University, Rokkodai, Nada, Kobe 657-8501, Japan